

# A high-power narrow-linewidth 1018 nm fiber laser based on a single-mode–few-mode–single-mode structure

Man Jiang, Pu Zhou, Hu Xiao, and Pengfei Ma

College of Optoelectronic Science and Engineering, National University of Defense Technology, Changsha 410073, China

(Received 8 March 2015; revised 8 June 2015; accepted 2 July 2015)

## Abstract

We demonstrate an all-fiber high-power Yb-doped 1018 nm fiber laser with a Gaussian-shaped output beam profile based on a mismatched structure, which consists of a pair of single-mode fiber Bragg gratings and a section of few-mode double-cladding gain fiber. The output power is up to 107.5 W with an optical-to-optical efficiency of 63%, and the 3 dB band is 0.26 nm at this power level. Such a structure of single-mode–few-mode–single-mode fiber oscillator can be used to generate high-power narrow-linewidth lasing with excellent beam quality in other spectral ranges.

**Keywords:** fiber laser; 1018 nm laser

## 1. Introduction

Yb-doped fiber (YDF) has attracted attention in the past decade due to its excellent capability in high-power output with good beam quality in a wide spectral range from 0.98 to 1.2  $\mu\text{m}$  theoretically<sup>[1, 2]</sup>. Researchers have taken more and more interest in narrow-linewidth YDF lasers (YDFs) within the short-wavelength range because they have extensive applications. For example, YDFs at wavelength ranges of 1010–1020 nm with narrow bandwidths can not only be frequency quadrupled to  $25\times$  nm for laser-induced fluorescence, optical refrigeration, semiconductor inspection and atomic trapping applications<sup>[3–7]</sup> but can also be used for tandem-pumping high-power C-band (1.06–1.12  $\mu\text{m}$ ) YDFs, due to their smaller quantum defect which gives higher conversion efficiency and lower thermal load<sup>[8, 9]</sup>. Moreover, as an outstanding pathway for achieving scalable high-power lasers with good beam quality, spectral beam combining (SBC) combines multiple lasers into a single beam for maximum output power<sup>[10–17]</sup>. To date, the most common wavelength range for SBC is from 1050 to 1080 nm. High-power narrow-linewidth short-wavelength lasers will broaden out the spectral range of SBC from 1010 to 1080 nm, which is twice as large as it was before.

Several narrow-linewidth YDFs within short wavelength ranges have been reported recently. In 2006, Seifert *et al.*

showed an efficient, narrow-linewidth, two-stage fiber amplifier at 1014.8 nm with 5 W output power based on Yb-doped double-clad fibers<sup>[18]</sup>. In 2013, Mo *et al.* exhibited a 164 mW linearly polarized low-noise single-frequency fiber laser at 1014 nm based on a 5 mm-long Yb-doped phosphate fiber<sup>[19]</sup>. In the same year, Hu *et al.* demonstrated an 8 W continuous-wave linearly polarized single-frequency 1014.8 nm fiber amplifier working at room temperature<sup>[20]</sup>. Recently, Hu *et al.* reported a single-frequency 1014.8 nm YDF amplifier with 19.3 W output power<sup>[21]</sup>. Beier *et al.* reported a single-mode continuous-wave fiber laser amplifier emitting 146 W output power at a wavelength of 1009 nm with bulk optics<sup>[22]</sup>. However, the net gain of YDF in the shorter wavelength range, such as 1010–1020 nm, is relatively smaller than that in the longer wavelength range, such as 1030–1040 nm, as the absorption cross section of YDF in the shorter wavelength range is larger than that in the longer wavelength range. Consequently, shorter wavelength lasers would act as pump sources to produce amplified spontaneous emission (ASE) near  $\sim 1030$  nm wavelength, which is the essential challenge to generate high-power good-beam-quality lasing in shorter wavelength ranges<sup>[9]</sup>. In order to obtain high-power lasing in a short spectrum with proper active fiber length, multimode fibers with large ratios of core/cladding diameters have been used. The disadvantage of these gain fibers is that they destroy the condition of  $V < 2.405$ , leading to a degraded beam quality. According to  $V = 2\pi/\lambda_0 \times a \times \text{NA}$ <sup>[23]</sup>, in which  $V$  is the normalized frequency  $V$ -number of the fiber,  $\lambda_0$  is the wavelength of

Correspondence to: P. Zhou, College of Optoelectronic Science and Engineering, National University of Defense Technology, Changsha 410073, China. Email: [zhoupu203@163.com](mailto:zhoupu203@163.com)



**Figure 1.** Brief schematic diagram of the 1018 nm fiber laser. HR, high-reflectivity; LR, low-reflectivity; FM-YDF, few-mode Yb-doped fiber.

the light transmitted in vacuum,  $a$  is the radius of the fiber core and NA represents the numerical aperture of the fiber, only if  $V < 2.405$  will the lasing in the oscillator maintain single-mode operation; otherwise high-order modes will be excited in the oscillator. For some multimode fibers, core/cladding diameters of 15/130  $\mu\text{m}$ , 20/130  $\mu\text{m}$  or even 30/130  $\mu\text{m}$  are offered to improve the absorption of pump power; but  $V < 2.405$  means that the NA must be lower than 0.05 (@ core/cladding diameter of 15/130  $\mu\text{m}$ ) for 1010–1020 nm fiber lasers. However, due to the fabrication limits, it is difficult to reduce the NA of a step-index fiber to lower than 0.06<sup>[24]</sup>. Specially designed photonics crystal gain fibers also appear to achieve high-power lasing with good beam quality<sup>[25]</sup>. However, their splicing with other kinds of commercial fibers is rather complicated. To achieve a high-power fiber laser while maintaining excellent beam quality in the shorter wavelength range, we propose a mismatched structure based on a single-mode–few-mode–single-mode (SFS) fiber configuration. The laser cavity is formed by a pair of fiber Bragg gratings (FBGs) written in single-mode fibers, and the gain medium employs a section of few-mode active fiber. In such a structure, the few-mode active fiber can improve the absorption of pump power, leading to a higher output power than a single-mode gain fiber, and the pair of single-mode FBGs can limit the output beam in one mode and guarantee perfect beam quality of the output laser. This design comes from the all-fiber multimode interference bandpass filter that was reported in 2006<sup>[26]</sup>. By employing a single-mode–multimode–single-mode (SMS) structure, J. Zhou *et al.* demonstrated an all-fiber Yb-doped laser operating at 1088 nm with an output power of up to 38.5 W<sup>[24]</sup>.

By using the SFS mismatched structure design, we demonstrate a high-power narrow-linewidth YDFL in the 1018 nm wavelength range with a Gaussian-shaped output beam profile. An optical-to-optical efficiency of 63% is achieved at the highest output power of up to 107.5 W, and the 3 dB bandwidth of this short-wavelength fiber laser is only 0.26 nm at 100 W lasing output.

## 2. Experimental setup and results

The experimental setup is shown in Figure 1. The emissions of four 976 nm laser diodes (LDs) are launched into the laser cavity through a pump combiner. The linear laser cavity consists of a pair of FBGs with reflectivities of

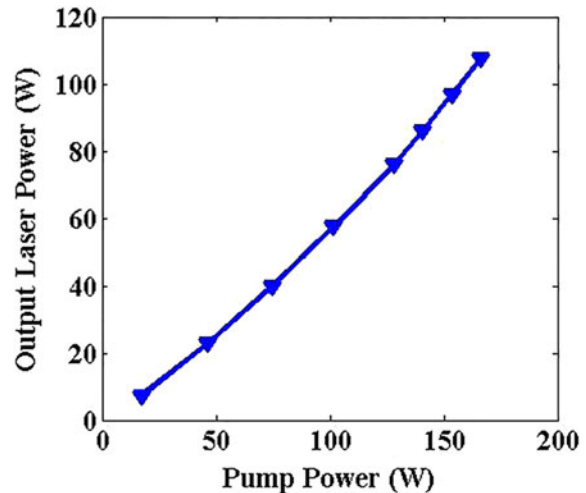


**Figure 2.** Laser output power versus pump power of the SFS-YDFL.

approximately 99.8% and 10%, respectively. Both of the central wavelengths of these two FBGs are located near 1018 nm with 3 dB bandwidths of approximately 1.3 and 0.7 nm, respectively. A section of optimized length 3.7 m with core/cladding diameters of 15/130  $\mu\text{m}$  double-cladding YDF is spliced between the two FBGs recorded in single-mode fibers with core/cladding diameters of 10/125  $\mu\text{m}$ . The low-reflectivity FBG acts as the output coupler (OC), which is angle cleaved to suppress the backward reflection. Consequently, the SFS mismatched structure is formed. The cladding absorption coefficient of the 15/130-YDF is approximately 6 dB/m at 976 nm, which is higher than that of a single-mode YDF (approximately 4 dB/m). Therefore, one can reduce the length of the active fiber to restrain ASE in the longer wavelength range as well as assuring sufficient absorption of the pump light and higher power output of the lasing light. The NA of the YDF is 0.08, resulting in  $V = 3.7$  ( $2 \times a = 15 \mu\text{m}$ ,  $\lambda_0 = 1018 \text{ nm}$ ), which supports the existence of two modes:  $\text{LP}_{01}$  and  $\text{LP}_{11}$ . On the other hand, the pair of 10/125  $\mu\text{m}$  single-mode FBGs will select and ensure the fundamental mode transmission only. In this experiment, light from the high-reflectivity FBG with a single mode couples into the few-mode active fiber, stimulating two modes, and then transmits to the OC FBG, back into one mode. Thus, an output laser with perfect beam quality can be expected.

Figure 2 shows the output power of the 1018 nm SFS fiber laser rising up as a function of the pump power added. The output power emitted from the laser cavity is up to 107.5 W. It is found that the slope efficiency of the power curve climbs as the pump power increases. This is because in this experiment, at lower pump current, the pump wavelength deviates from 976 nm, which is the absorption peak of  $\text{Yb}^{3+}$  ions. The diode laser spectrum shifts to  $\sim 976 \text{ nm}$  because the temperature goes up with the pump current enhanced. Thus, by properly controlling the temperature of the LDs and

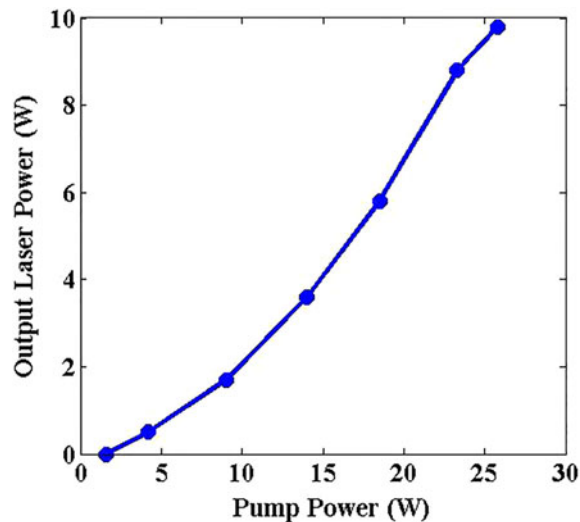


**Figure 3.** Laser output power versus pump power of the 10/125  $\mu\text{m}$  fiber laser.

causing the pump wavelength to be centered at 976 nm, one can use the advantage of large pump absorption of the few-mode active fiber to build up the SFS structure and achieve high-power output with high efficiency.

For comparison, we have also established a fiber laser consisting of perfectly matched fibers. The geometric parameters of the gain fiber with core/cladding diameters of 10/125  $\mu\text{m}$  are nearly the same as those of the pigtailed fiber of the FBGs; this makes the laser have a single-mode output. Its cladding absorption coefficient is approximately 4 dB/m@976 nm. The segment length of this fiber is only 2.5 m, which has been optimized for suppressing ASE<sup>[27]</sup>. If a longer fiber length were employed, it would lead the oscillator to generate ASE in a longer wavelength range as well as self-excitation, which could ruin the devices of the cavity and the pump source. However, the average slope efficiency will be compromised due to the insufficient absorption of pump power. Figure 3 plots the power properties of this laser. Meanwhile, in the 15/130  $\mu\text{m}$  double-cladding YDFL experiment, a longer section of YDF could be employed (3.7 m) as its higher core–cladding ratio leads to a stronger absorption coefficient than 10/125  $\mu\text{m}$  YDF. Therefore, a proper length of 15/130  $\mu\text{m}$  YDF with sufficient absorption at the pump wavelength could ensure high-power operation and suppress ASE simultaneously. It is apparent that the SFS mismatched structure fiber laser exhibits better performance in its high efficiency and power scaling ability while maintaining good beam quality.

The output laser beam of the SFS fiber laser has a Gaussian-shaped beam profile with good beam quality, as shown in Figure 4,  $M^2 < 1.1$ . Therefore, such a high-power high-brightness YDFL within short-wavelength ranges based on the SFS structure would act as an excellent pump source for tandem-pumping high-power C-band fiber lasers.

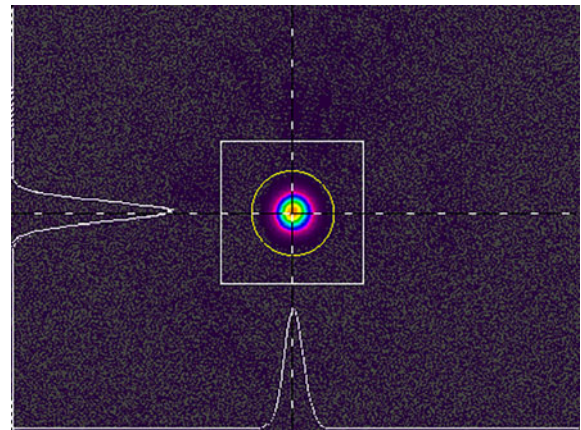


**Figure 4.** Far-field output beam profile of the 1018 nm SFS-YDFL.

Further power scaling of this short-spectral-range YDFL is limited by the pump power of the LDs.

Figure 5 plots the output spectral characteristics at the maximum output power. The peak spectrum is at 1018.26 nm and there is no evident pump power or ASE in the spectrum, indicating that the parameters of the YDF are appropriate to absorb the pump power adequately and suppress ASE at this power level. The spectral bandwidth extends slightly when the output power increases. Figure 5(b) shows the spectral shape of this oscillator at 100 W output power in linear coordinates. The 3 dB band at 100 W output power is only 0.26 nm. This type of narrow-band YDFL can be used for high-power SBC, because the narrow bandwidth of the SFS-YDFL is under the nanometer class, which can meet the demands of SBC<sup>[28]</sup>. It is indicated that based on the SFS structure, short-wavelength YDFs would expand the spectral range of SBC from the 1050–1080 nm band to the 1010–1080 nm band, and that shorter wavelength range combining would be achieved.

### 3. Conclusion

In this paper, a high-power narrow-linewidth 1018 nm YDFL with good beam quality based on the SFS mismatched structure is demonstrated. A section of 3.7 m 15/130  $\mu\text{m}$  double-cladding YDF spliced between a pair of FBGs recorded in single-mode fibers forms the SFS oscillator cavity. A maximum output laser power of up to 107.5 W with an optical-to-optical efficiency of 63% is obtained, and the 3 dB band at 100 W output power is 0.26 nm. We proved that the SFS structure can be used as an effective method to generate high-power high-brightness short-wavelength YDFs with narrow linewidths. The advantages of high power and good beam quality of this type of YDFL could be used to tandem-pump high-power C-band fiber lasers, and the narrow-linewidth short-wavelength light source is favorable for expanding the spectral range of SBC to be twice as wide

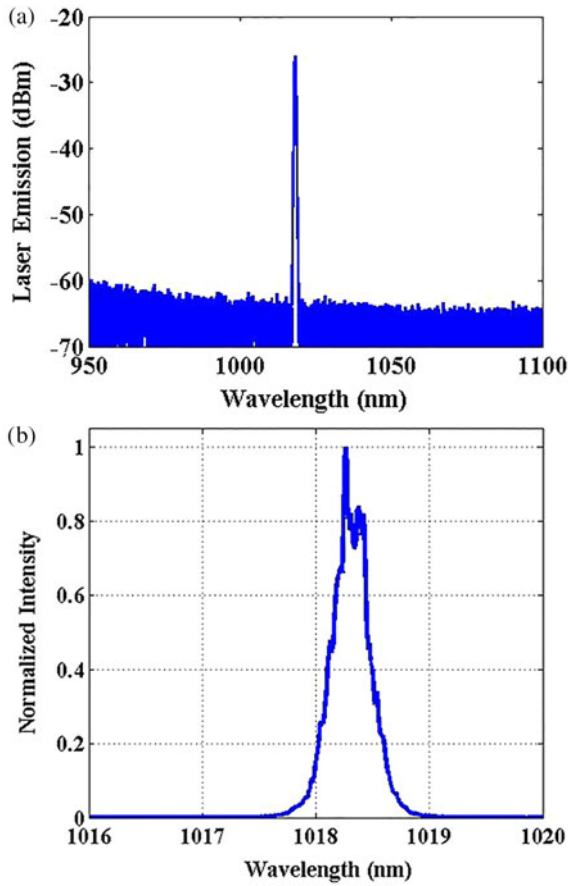


**Figure 5.** (a) Laser emission spectrum at different output powers, (b) laser emission spectrum at 100 W output power in linear coordinates.

as before. Furthermore, YDFs based on the SFS structure can also be used to generate high-power narrow-band lasing with excellent beam quality in other spectral ranges.

### Acknowledgements

This work is supported by the programme for New Century Excellent Talents in University and the Innovation Foundation for Postgraduate Student of the National University of Defense Technology.

### References

1. H. M. Pask, R. J. Carman, D. C. Hanna, A. C. Troppe, C. J. Mackechnie, P. R. Barber, and J. M. Dawes, *IEEE J. Sel. Top. Quantum Electron.* **1**, 2 (1995).
2. D. J. Richardson, J. Nilsson, and W. A. Clarkson, *J. Opt. Soc. Am. B* **27**, B63 (2010).

3. R. Steinborn, A. Koglbauer, P. Bachor, T. Diehl, D. Kolbe, M. Stappel, and J. Walz, *Opt. Express* **21**, 22693 (2013).
4. A. T. Case, D. Tan, R. E. Stickel, and J. Mastromarino, *Appl. Opt.* **45**, 2306 (2006).
5. L. Yi, S. Mejri, J. J. MeFerran, Y. LeCoq, and S. Bize, *Phys. Rev. Lett.* **106**, 073005 (2011).
6. M. Ostermeyer, P. Kappe, R. Menzel, and V. Wulfmeyer, *Appl. Opt.* **44**, 582 (2005).
7. P. Villwoek, S. Siol, and T. Walther, *Eur. Phys. J. D* **65**, 251 (2011).
8. H. Injeyan and G. D. Goodno, *High-Power Laser Handbook* (The McGraw-Hill Companies, Inc., 2011).
9. Y. Huang, J. Edgecumbe, J. Ding, R. Holten, P. Ahmadi, C. Wang, C. Guintrand, K. Farley, S. Christensen, and K. Tankala, *Proc. SPIE* **8961**, 89612K (2014).
10. S. J. Augst, J. K. Ranka, T. Y. Fan, and A. Sanchez, *J. Opt. Soc. Am. B* **24**, 1707 (2007).
11. D. R. Drachenberg, O. Andrusyak, I. Cohanoschi, I. Divliansky, O. Mokhun, A. Podvyaznyy, V. Smirnov, G. B. Venus, and L. B. Glebov, *Proc. SPIE* **7580**, 75801U (2010).
12. D. Drachenberg, I. Divliansky, V. Smirnov, G. Venus, and L. Glebov, *Proc. SPIE* **7914**, 79141F (2011).
13. C. Wirth, O. Schmidt, I. Tsybin, T. Schreiber, T. Peschel, F. Brückner, T. Clausnitzer, J. Limpert, R. Eberhardt, A. Tünnermann, M. Gowin, E. ten Have, K. Ludewigt, and M. Jung, *Opt. Express* **17**, 1178 (2009).
14. C. Wirth, O. Schmidt, I. Tsybin, T. Schreiber, R. Eberhardt, J. Limpert, A. Tünnermann, K. Ludewigt, M. Gowin, E. ten Have, and M. Jung, *Opt. Lett.* **36**, 3118 (2011).
15. T. H. Loftus, A. M. Thomas, P. R. Hoffman, M. Norsen, R. Royse, A. Liu, and E. C. Honea, *IEEE J. Sel. Top. Quantum Electron.* **13**, 487 (2007).
16. T. H. Loftus, A. Liu, P. R. Hoffman, A. M. Thomas, M. Norsen, R. Royse, and E. Honea, *Opt. Lett.* **32**, 349 (2007).
17. R. S. Afzal, E. Honea, M. S. Leuchs, N. Gitkind, R. Humphreys, J. Henrie, K. Brar, and D. Jander, *Proc. SPIE* **8547**, 854706 (2012).
18. A. Seifert, M. Sinther, T. Walther, and E. S. Fry, *Appl. Opt.* **45**, 7908 (2006).
19. S. Mo, S. Xu, X. Huang, W. Zhang, Z. Feng, D. Chen, T. Yang, and Z. Yang, *Opt. Express* **21**, 12419 (2013).
20. J. Hu, L. Zhang, H. Liu, K. Liu, Z. Xu, and Y. Feng, *Opt. Express* **21**, 30958 (2013).
21. J. Hu, L. Zhang, H. Liu, K. Liu, Z. Xu, and Y. Feng, *Appl. Opt.* **53**, 4972 (2014).
22. F. Beier, H. J. Otto, C. Jauregui, O. de Vries, T. Schreiber, J. Limpert, R. Eberhardt, and A. Tünnermann, *Opt. Lett.* **39**, 3725 (2014).
23. G. Brooker, *Modern Classical Optics* (Oxford University, 2003), p. 316.
24. J. Zhou, B. He, Y. Feng, and X. Gu, *Appl. Opt.* **53**, 5554 (2014).
25. J. He, S. Du, Z. Wang, J. Zhou, and Q. Lou, *Opt. Express* **21**, 29240 (2013).
26. W. S. Mohammed, P. W. E. Smith, and X. Gu, *Opt. Lett.* **31**, 2547 (2006).
27. H. Xiao, P. Zhou, X. Wang, S. Guo, and X. Xu, *IEEE Photon. Technol. Lett.* **24**, 1088 (2012).
28. P. Madasamy, D. R. Jander, C. D. Brooks, T. H. Loftus, A. M. Thomas, P. Jones, and E. C. Honea, *IEEE J. Sel. Top. Quantum Electron.* **15**, 337 (2009).